Short Term Mild Traumatic Brain Injury Mechanisms Characterized in an *in vivo* Göttingen Minipig Model

E. M. Fievisohn[1], V. S. Sajja[1], B. M. Vaughn[1], P. J. VandeVord[1, 2], and W. N. Hardy[1]
[1]Virginia Tech-Wake Forest University, Center for Injury Biomechanics; [2]Salem VA Medical Center, Research & Development Service

ABSTRACT

Traumatic brain injury (TBI) is a recurring problem with an estimated 1.7 million occurrences annually in the United States, accounting for 30.5% of all injury-related deaths (CDC, 2010). This study seeks to answer many of the unknowns surrounding mild TBI (mTBI) regarding the mechanisms and pathogenesis involved over 24 hours by using magnetic resonance spectroscopy (MRS) and immunohistochemistry (IHC). A repeatable rotational injury device was used to induce mTBI in Göttingen minipigs. The minipigs underwent baseline MR scans (7T Bruker) prior to injury and twenty-four hours post injury, at which point the brains were perfused and harvested for IHC. MRS was used to quantify metabolites in a 216 mm^3 voxel placed in the genu of the corpus callosum. Metabolites of interest included glutamate (Glu), N-acetylaspartate (NAA), N-acetylaspartylglutamate (NAAG), glutamine (Gln), and the combination of Glu+Gln. IHC was performed on the genu with four antibodies; light neurofilament (LNF), heavy neurofilament (HNF), glial fibrillary acid protein (GFAP), and cleaved caspase-3. ImageJ was used to calculate integrated density for comparison between groups. Two 24 hour sham control and eight 24 hour rotational injury animals have been tested. Three animals have been dropped from an angle of 15° and 25°, one from 35° and one from 40°. Paired Student's t-tests yielded significant increases in Glu+Gln, Glu/Gln, Glu/NAAG, NAA/NAAG, and Glu+Gln/NAAG between all baseline and 24 hour post injury concentrations ($p<0.05$). IHC analysis with two tailed Student's t-tests identified a significant increase in LNF and HNF ($p<0.05$) build-up between sham and injury animals ($p<0.05$). GFAP and cleaved caspase-3 stains were not significant between sham and injury animals. In conclusion, there are significant differences that can be seen using MRS and IHC within 24 hours. Next, the staining results will be correlated with the MRS results. This will facilitate interval MRS scanning during a subsequent longitudinal study of the time course development of mTBI.

2013 Ohio State University Injury Biomechanics Symposium
This paper has not been peer-reviewed.

INTRODUCTION

Traumatic brain injury (TBI) remains a concern in society with approximately 1.7 million occurrences annually in the United States (CDC, 2010), despite a wide range of research dedicated to understanding, intervention, and prevention. Animal models are frequently used to investigate the pathology and mechanisms associated with TBI. Some of the more popular injury models include fluid percussion (Lindgren and Rinder, 1966), weight drop (Denny-Brown and Russell, 1941; Scott, 1940), controlled cortical impact (Lighthall, 1988), and inertial rotation (Unterharnscheidt and Higgins, 1969). These models were studied *in vivo* in mostly rats (Xiong et al., 2013), with some studies involving animals with a more complex brain such as swine (Meaney et al., 1993; Manley et al., 2006; Armstead and Kurth, 1994) and monkeys (Adams et al., 1981; Gennarelli et al., 1981). However, there are limitations with these methods, specifically using a rodent animal model and also with the overall mechanics of the injury devices. Two main causes of TBI are motor vehicle accidents and falls (Bruns and Hauser, 2003) which are mostly non-penetrating and impact based in nature. This fact makes the fluid percussion and controlled cortical impact clinically irrelevant due to the need for a craniotomy. The inertial rotation device does not require a craniotomy, but produces a non-impact based injury. The weight drop models do mimic an impact based injury and do not require a craniotomy, however the design of the device does not allow for direct measurement of the input kinematics, does not produce repeatable results (Marmarou et al., 1994; Xiong et al., 2013), and the device has mostly been tested on rodents (Xiong et al., 2013) which have a brain dissimilar to that of humans (Swanson, 1995). No experimental paradigm exists that is capable of successfully addressing prevention, intervention, and/or treatment, providing the impetus for a new approach to studying TBI.

This proposed study moves away from previous traumatic brain injury models to study injury mechanisms using an impact based rotational injury device. Göttingen minipigs were selected due to the gyrencephalic nature of the minipig brain (Jelsing et al., 2005), the pronounced falx cerebri, and that the brainstem exits at an angle closer to a human than other animal models (Fievisohn et al., 2012). Both immunohistochemistry and a noninvasive magnetic resonance spectroscopy (MRS) metabolite measurement were used to characterize the injury in the corpus callosum, a region found to be one of the most injured parts of the brain after road fatalities (Adams et al., 1985; Gorrie et al., 2001).

METHODS

Ten female Göttingen minipigs (Marshall Bioresources, North Rose, NY) (~5 months old, weighing ~10kg, approximating a young adult) were divided into sham (n=2) and 24 hour survival rotational injury animals (n=8) with three dropped from an angle of 15°, three from 25°,

one from 35°, and one from 40°. The animal protocol was approved by the Wake Forest University Baptist Medical Center's Animal Care and Use Committee.

Animals were sedated with an oral dose of midazolam (1 mg/kg) before being anesthetized with 3-5% isoflurane for induction and 1.5-2% maintenance. Intravenous fluids were administered through an ear catheter.

All animals (including shams) underwent head surgical preparation. The incision site was shaved and scrubbed three times alternating with alcohol and betadine. Bupivacaine (0.25%) was given subcutaneously around the incision site serving as a local anesthetic while Buprenorphine (0.05 mg/kg) was given intramuscularly for analgesia. A cruciate incision was made and the skin reflected away. Six small pieces of periosteum were dissected away so that custom bone screws, that do not penetrate the inner table, could be inserted into the skull. A sterile dental dam was used to create a barrier between the skull and Bosworth Trim® dental cement (Bosworth® Company, Illinois). The dental cement was used to connect the bone screws to a steel slug. This steel slug was bolted into the injury device which guaranteed a rigid connection between the animal and the device (Figure 1).

Figure 1: Steel slug and bone screws cemented to the minipig skull (left) and minipig bolted into the injury device and restrained (right).

The rotational injury device (Figure 2) consists of two aluminum plates that can rotate with respect to one another. It lifts up to a desired angle and then drops onto brass tubing that controls the acceleration pulse and ensures a repeatable impact.

The animals were fixed to the injury device in the supine position. A restraint system (Figure 2) was used to prevent any undesirable decoupling or injury from occurring. The steel slug cemented to the minipig skull was bolted into a steel cube that hosts the instrumentation, and impacts the brass tubing, causing repeatable rapid deceleration of the animal. Instrumentation consisted of two linear accelerometers (7264-3000TZ-360), one angular accelerometer (7302BM4) (Meggitt Sensing Systems, San Juan Capistrano, CA), and one angular rate sensor (ARS PRO, DTS, Seal Beach, CA). A TDAS Pro 4M rack was used for data acquisition at 20 kHz (DTS, Seal Beach, CA). Data is represented as average linear acceleration, rotational speed, and rotational acceleration. High speed video was used for overall observation (HHC X3, Mega Speed USA, San Jose, CA).

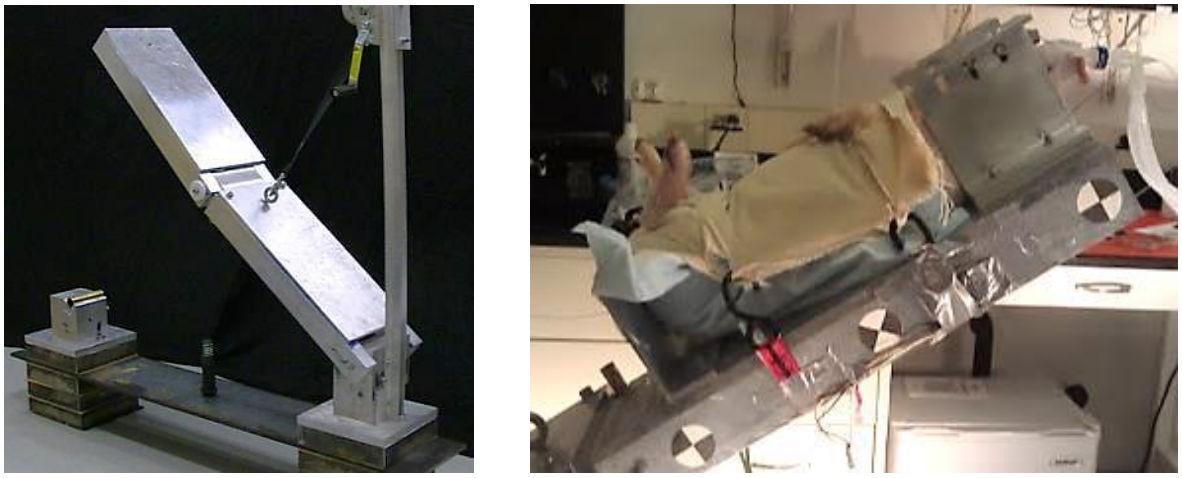

Figure 2: Rotational injury device (left) and with a minipig bolted and restrained (right) (Fievisohn et al., 2012).

Magnetic Resonance Spectroscopy

MRS was carried out using a 7T Bruker Biospin MR scanner at the Center for Biomolecular Imaging at the Wake Forest University Baptist Medical Center. A custom two-channel quadrature coil enables proper tuning and positioning of the minipig head as described in Fievisohn et al., 2012. After the 1600 signal averages were taken in a 216 mm^3 voxel (Figure 3) placed in the genu of the corpus callosum, LCModel (Stephen Provencher Inc. Oakville, Ontario, CA) resolved the metabolites into concentrations (mM). Water scaling was used to obtain absolute metabolite concentrations including alanine, aspartate, creatine (Cr), phosphocreatine (PCr), γ-aminobutyric acid, glucose, glutamine (Gln), glutamate (Glu), glycerylphosphocholine (GPC), phosphorylcholine (PCh), myo-inositol (Ins), lactate, n-acetylaspartate (NAA), n-acetylaspartateglutamate (NAAG), scyllo, taurine, guanine, and combinations of more than one metabolite such as GPC+PCh, NAA+NAAG, Cr+PCr, and Glu+Gln. MRS scans were taken at baseline and 24 hours after injury.

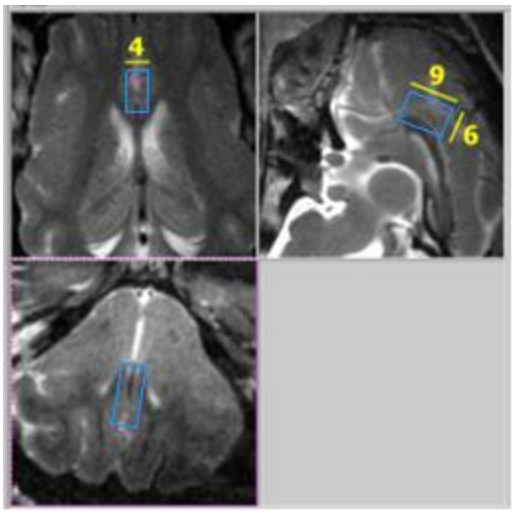

Figure 3: 216 mm^3 voxel placement in the genu of the corpus callosum with the voxel being 4 mm left-right, 9 mm anterior-posterior, and 6 mm head-foot.

Metabolite concentrations were analyzed using paired Student's t-tests that compared differences between baseline and 24 hour values for NAA, NAAG, Glu, Gln, Glu+Gln, but also looking at the ratios Glu/Gln, Glu/NAAG, NAA/NAAG, and Glu+Gln/NAAG. A p-value less than 0.05 was considered statistically significant. Data is represented as average ± standard deviation.

Immunohistochemistry

After the 24 hour post-injury scanning was completed, the brains were perfused with 4% paraformaldehyde and harvested. The genu of the corpus callosum was embedded in paraffin wax and then sectioned using ~4 μm slices.

Injury characterization was determined using immunofluorescent staining which identified axonal damage by highlighting light and heavy neurofilament, astrocyte activation by binding with glial fibrillary acid protein (GFAP), and apoptosis by labeling with cleaved caspase-3.

Briefly, paraffin slides were first deparaffinized in xylene twice for five minutes, then hydrated with 100% ethanol twice for three minutes and in 95% ethanol for one minute. The slides were then rinsed in distilled water and placed in a microwavable vessel containing sodium citrate buffer. The slides were heated until the solution boiled and then for an additional 20 minutes. Slides were cooled with running distilled water for 10 minutes. The slides were then washed thoroughly in phosphate-buffered saline (PBS) three times for five minutes each. A 0.5% blocking buffer was added and the slides were incubated for one hour. Primary antibody solution was added subsequently at a concentration of 1:100 for light and heavy neurofilament (anti-68 kDa and anti-200 kDa, Abcam®, Cambridge, MA) for one set of slides, and for GFAP and Caspase-3 (anti-GFAP and anti-Caspase 3, Abcam®, Cambridge, MA) for another set of slides.

The slides were incubated in primary antibody solution overnight at 4°C. Then, the slides were rinsed in PBS three times for five minutes each. Next, secondary antibody was added at a concentration of 1:100 to fluorescently label the light neurofilament of one set of stained slides and GFAP of the other with fluorescein isothiocyanate (FITC) or a green color (FITC-AffiniPure Donkey Anti-Mouse IgG, Jackson ImmunoResearch Laboratories Inc, West Grove, PA). A secondary antibody tagged with alexa fluor or a red color (Alexa Fluor 555 Donkey Anti-Rabbit IgG, Life Technologies™, Grand Island, NY) was used to label the heavy neurofilament of one set of stained slides and Caspase-3 of the other set. After the slides were incubated at room temperature in secondary antibody for 1.5 hours, the slides were washed in PBS three times for five minutes each. The slides then dried before SlowFade® Gold anti-fade reagent with DAPI (Life Technologies™, Grand Island, NY) was used to label cell bodies with DAPI (4', 6-diamidino-2-phenylindole) or a blue color and coverslips were applied.

Images were taken with a Zeiss Axiovert 40 CFL (Carl Zeiss Microscopy, Oberkochen, Germany). Three to five images were taken in the genu of the corpus callosum which is assumed to represent the distribution of stain throughout the entire region. The images were taken at a magnification of 20x resulting in an image area of 1392 mm x 1038 mm.

ImageJ (NIH, Bethesda, Maryland) was used to calculate integrated density. Thresholds were set based on the images from the sham animals for each colored stain. A macro routine was used to automate the process to eliminate user bias. The integrated density over the images per animal per slide (n=2 slides per animal) was averaged to get a final integrated density for each animal. Two tailed Student's t-tests were used to compare sham animal average integrated densities to all 24 hour injury average integrated densities. Comparisons were not made between injury severities due to the small sample size. A p-value less than 0.05 was considered statistically significant.

RESULTS

Table 1 shows the input kinematics measured for each injury event. These include average rotational and linear acceleration and angular speed for each of the drop height.

Table 1: Average peak linear acceleration, rotational acceleration, and rotational speed for tests at the different drop heights

Drop Height	n	Avg. Peak Linear Acceleration (G's)	Avg. Peak Rotational Speed (rad/s)	Avg. Peak Rotational Acceleration (rad/s^2)
15°	3	43	8	1800
25°	3	63	10	2000
35°	1	81	11	2500
40°	1	103	11.5	3300

Magnetic Resonance Spectroscopy

Significant increases ($p<0.05$) were found at the 24 hour time point for all injured animals compared to their baseline concentrations for Glu, Glu+Gln, and in the ratios of Glu/Gln, Glu/NAAG, NAA/NAAG, and Glu+Gln/NAAG. NAA concentrations were trending toward statistical significance with $p=0.052$ (Table 2).

Table 2: Metabolite comparisons between baseline and 24 hour concentrations (*$p<0.05$)

	Baseline (mM)	24 hour (mM)	p-value
NAA	5.24±0.71	6.35±1.26	0.052
NAAG	3.37±1.76	1.96±0.64	0.09
NAA+NAAG	7.75±1.12	8.12±0.76	0.28
Glu	6.28±1.44	7.81±2.32	0.01*
Gln	5.71±1.84	6.22±1.60	0.30
Glu+Gln	11.28±3.29	14.80±1.47	0.022*
Glu/Gln	1.22±0.42	1.47±0.42	0.04*
Glu/NAAG	2.54±1.35	4.31±2.08	0.021*
NAA/NAAG	2.15±1.08	3.59±1.63	0.03*
Glu+Gln/NAAG	4.40±2.20	8.09±2.27	0.015*

Immunohistochemistry

There was a significant increase in the expression of light and heavy neurofilament (markers of axonal damage, Figure 4) due to the presence of injury ($p<0.05$). A trend in increased GFAP expression levels (a marker of astrocyte activation, Figure 5) in all of the injured animals was observed ($p=0.058$). No changes were observed in cleaved caspase-3.

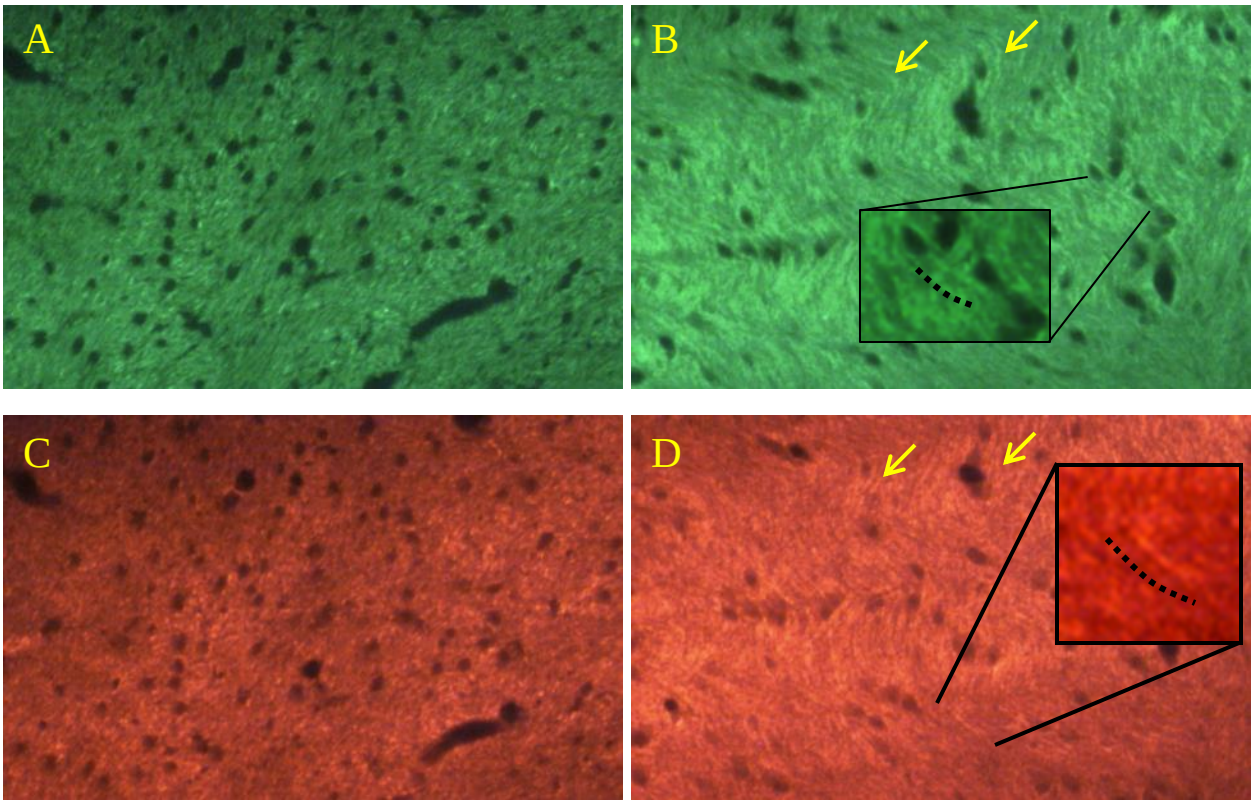

Figure 4: Representative images of the corpus callosum stained with light neurofilament (green) and heavy (red) between a sham (A, C) and an injured (B, D) animal. Short tracks of axonal damage identified by neurofilament staining are indicated by arrows and in the magnified window showing a dotted line alongside a stained axonal track.

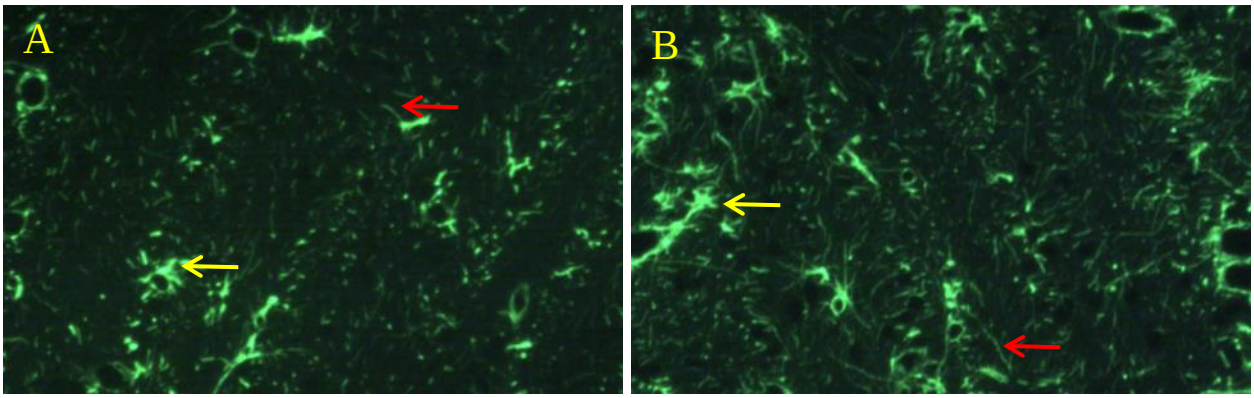

Figure 5: Representative images of GFAP staining between a sham (A) and an injured (B) animal. A slight increase in astrocyte activation can be seen in the injury image with the yellow arrows indicating an activated astrocyte and with the red arrows showing astrocyte processes which appear as lines of stain in the background.

DISCUSSION

Immunohistochemistry

Clinical axonal injury has been an indicator of TBI, specifically looking at the increased expression of light and heavy neurofilament. Previously, Ross et al., 1994 and Smith et al., 1998 found neurofilament buildup in Hanford minipigs due to inertial rotation injury. In addition, studies have found an increase in GFAP expression levels, which is a marker of astrocyte activation (Smith et al., 1997). Similarly, increased light and heavy neurofilament levels were observed in this study. An increased GFAP expression was trending towards significance due to injury ($p=0.058$). This could be an indicator of early inflammation in the corpus callosum due to damaged axons (Myer et al., 2006). Cleaved caspase-3 levels (a marker of apoptosis) were not significantly different between sham and injured groups in the genu of the corpus callosum. Since this region is predominately white matter, further study is needed to evaluate apoptotic response after injury.

Magnetic Resonance Spectroscopy

MRS data showed an increase in Glu and NAA, and decrease in NAAG levels. It is possible that NAAG is being hydrolyzed by the enzyme glutamate carboxypeptidase II (GCPII) to yield NAA and Glu. Significant increases in the ratios of Glu/NAAG and NAA/NAAG support this theory. In addition, an increase in the levels of Glu/Gln suggests a compromise in the primary metabolic pathway for the degradation of Glu (Patel et al., 2005). Excess Glu is an indicator of excitotoxicity (Ashwal et al., 2004) and has been observed in various neurodegenerative pathologies (Neale et al., 2005).

Further, the MRS data indicate a possibility of NAAG being broken down to release Glu as a product. NAAG's normal function of activating the $mGlu_3$ receptors on axon terminals inhibiting the release of Glu could be dysfunctional. This proposed pathway and the interaction between NAAG, NAA, and Glu is described by Figure 6. This is further supported by the axonal disruption observed using light and heavy neurofilaments affecting NAAG mechanistic regulation (Vrenken et al., 2005). In addition, a model proposed by Neale et al., 2005 supports drug treatments that will inhibit GCP II which will prevent the degradation of NAAG thereby reducing excitotoxic levels of Glu. Similar trends observed in this study with NAAG regulation leads to the speculation that GCP II could be essential in TBI etiology. Further study is needed to confirm these hypotheses.

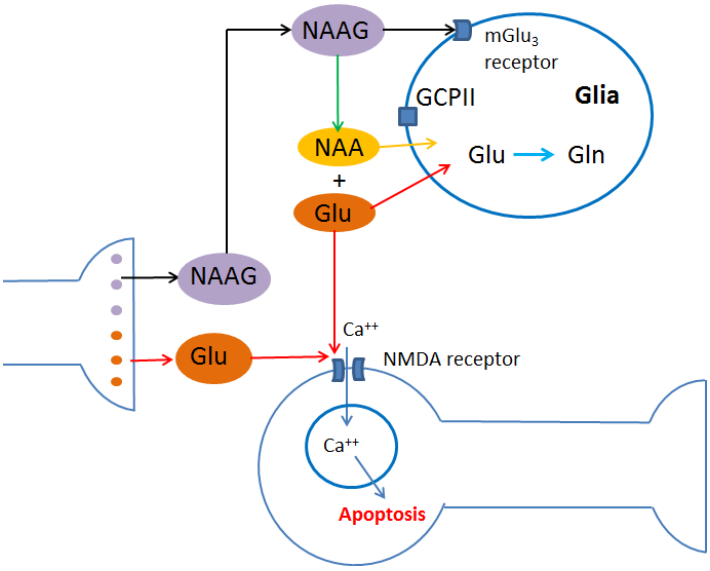

-The pathway involving NAAG activating $mGlu_3$ receptors thereby inhibiting further Glu release by the glial cells is compromised (black arrow). Instead it is being broken down to NAA and Glu by GCPII (green arrow). Excess Glu is excitotoxic and causes apoptosis (red arrows).

-Glu inactivated in glia by conversion to Gln (not detrimental).

-NAA stored in glia until released for uptake into neurons for NAAG synthesis or for the synthesis of myelin lipids in oligodendrocytes (not detrimental).

Figure 6: Hypothesized interactions between NAAG, NAA, and Glu between neurons and glia cells in the brain after (Neale et al., 2005) (Patel et al., 2005) (Benarroch, 2008).

Future work will include correlation analyses to see if the increases in staining are correlated with metabolite concentration differences, in addition to examining other metabolite relationships such as creatine and choline ratios. One of the goals of this study is to continue the spectral analyses, over the course of two weeks or more. Initial correlation of staining with metabolite concentrations will facilitate interval MRS scanning over time to evaluate damage instead of performing immunohistochemical analysis. In addition, behavioral testing will be added to look at function neurological deficit over the course of time.

Once the mapping of neuronal damage to metabolite concentration changes is completed over time, high-speed biplane x-ray studies looking at head kinematics, brain response, intracranial pressure, and brain injury will support the development of an FE model of the minipig head. Once validated, the model can be used to scale graded injury metrics for prediction of brain injury in the human. Ultimately, a new head injury criterion will be developed for better prediction of the potential for traumatic brain injury.

CONCLUSIONS

This study developed a new injury model to study impact induced mTBI. This new model is more representative of real-world impact than existing models. In addition, the animal used has a brain more similar to humans than the rodent brain. The device was designed to produce a repeatable impact for which the input kinematics are measured. Both MRS and

immunohistochemistry were used to show the presence of mild traumatic brain injury in the experimental animals. This was confirmed by statistically significant differences in light and heavy neurofilament and supported by a metabolite pathway described in the literature as causing excitotoxicity. Future work will lengthen this study over the course of two weeks in addition to adding a behavioral testing component. Initial testing for this injury model are encouraging, and ultimately will provide greater insight into directions that should be taken for prevention, intervention, and treatment of mTBI.

ACKNOWLEDGMENTS

This project was funded in part by the National Highway Traffic Safety Administration.

REFERENCES

ADAMS, J.H., DOYLE, D., GRAHAM, D.I., LAWRENCE, A.E., MCLELLAN, D.R., GENNARELLI, T.A., PASTUSZKO, M., SAKAMOTO, T. (1985). The Contusion Index: A Reappraisal in Human and Experimental Non-Missile Head Injury. Neuropathology and Applied Neurobiology, 11, 299-308

ADAMS, J.H., GRAHAM, D.I., GENNARELLI, T.A. (1981). Acceleration Induced Head Injury in the Monkey. II. Neuropathology. Acta Neuropathology Supplementum, 7, 26-28.

ARMSTEAD, W.M., KURTH, C.D. (1994). Different Cerebral Hemodynamic Responses Following Fluid Percussion Brain Injury in the Newborn and Juvenile Pig. Journal of Neurotrauma, 11, 487-497.

ASHWAL, S., HOLSHOUSER, B., TONG, K., SERNA, T., OSTERDOCK, T., GROSS, M., KIDO, D. (2004). Proton MR Spectroscopy Detected Glutamate/Glutamine is Increased in Children witth Traumatic Brain Injury. Journal of Neurotrauma, 21, 1539-1552.

BENARROCH, E.E. (2008). N-Acetylaspartate and N-acetylaspartylglutamate: Neurobiology and Clinical Significance. Neurology, 70, 1353-1357.

BRUNS, J., HAUSER, W.A. (2003). The Epidemiology of Traumatic Brain Injury: A Review. Epilepsia, 44, 2-10.

CENTERS FOR DISEASE CONTROL AND PREVENTION. Traumatic Brain Injury in the United States. 2002-2006. (2010).

DENNY-BROWN, D., RUSSELL, W.R. (1941) Experimental Cerebral Concussion. Brain, 64, 94-164.

FIEVISOHN, E.M., VAUGHN, B.M., HARDY, W.N. (2012). Techniques for the Investigation of Traumatic Brain Injury Mechanisms Characterized by Magnetic Resonance Spectroscopy. Biomedical Sciences Instrumentation, 48, 126-133.

GENNARELLI, T.A., ADAMS, J.H., GRAHAM, D.I. (1981). Acceleration Induced Head Injury in the Monkey. I. The Model, its Mechanical and Physiological Correlates. Acta Neuropathology Supplementum, 7, 23-25.

GORRIE, C., DUFLOU, J., BROWN, J., GIBSON, T., WAITE, P.M.E. (2001). Extent and Distribution of Vascular Brain Injury in Pediatric Road Fatalities. Journal of Neurotrauma, 18, 849-860.

JELSING, J., OLSEN, A.K., CUMMING, P., GJEDDE, A., HANSEN, A.K., ARNFRED, S., HEMMINGSEN, R., PAKKENBERG, B. (2005). A Volumetric Screening Procedure for the Göttingen Minipig Brain. Exp Brain Res, 162, 428-435.

LIGHTHALL, J.W. (1988). Controlled Cortical Impact: A New Experimental Brain Injury Model. Journal of Neurotrauma, 5, 1-15.

LINDGREN, S., RINDER, L. (1966). Experimental Studies in Head Injury II. Pressure Propagation in "Percussion Concussion". Biophysik, 3, 174-180.

MANLEY, G.T., ROSENTHAL, G., LAM, M., MORABITO, D., YAN, D., DERUGIN, N., BOLLEN, A., KNUDON, M.M., PANTER, S.S. (2006). Controlled Cortical Impact in Swine: Pathophysiology and Biomechanics. Journal of Neurotrauma, 23, 128-139.

MARMAROU, A., FODA, M.A.A.E., BRINK, W.V.D., CAMPBELL, J., KITA, H., DEMETRIADOU, K. (1994). A New Model of Diffuse Brain Injury in Rats, Part I: Pathophysiology and Biomechanics. Journal of Neurosurgery, 80, 291-300.

MEANEY, D.F., SMITH, D., ROSS, D.T., GENNARELLI, T.A. (1993). Diffuse Axonal Injury in the Miniature Pig: Biomechanical Development and Injury Threshold. AMD, 169: 169-175.

MYER, D.J., GURKOFF, G.G., LEE, S.M., HOVDA, D.A., SOFRONIEW, M.V. (2006). Essential protective roles of reactive astrocytes in traumatic brain injury. Brain, 129: 2761-2772.

NEALE, J.H., OLSZEWSKI, R.T., GEHL, L.M., WROBLEWSKA, B., BZDEGA, T. (2005). The Neurotransmitter N-acetylaspartylglutamate in Models of Pain, ALS, Diabetic Neuropathy, CNS Injury and Schizophrenia. TRENDS in Pharmcological Sciences, 26, 477-484.

PATEL, A.B., DEGRAAF, R.A., MASON, G.F., ROTHMAN, D.L., SHULMAN, T.G., BEHAR, K.L. (2005). The Contribution of GABA to Glutamate/Glutamine Cycling and Energy Metabolism in the Rat Cortex *in vivo*. PNAS, 102, 5588-5593.

ROSS, D.T., MEANEY, D.F., SABOL, M.K., SMITH, D.H., GENNARELLI, T.A. (1994). Distribution of Forebrain Diffuse Axonal Injury Following Inertial Closed Head Injury in Miniature Swine. Experimental Neurology, 126, 291-299.

SCOTT, W.W. (1940). Physiology of Concussion. Arch Neurol Psychiatry, 43, 270-283.

SMITH, D.H., CECIL, K.M., MEANEY, D.F., CHEN, X.H., MCINTOSH, T.K., GENNARELLI, T.A., LENKINSKI, R.E. (1998). Magnetic Resonance Spectroscopy of Diffuse Brain Trauma in the Pig. Journal of Neurotrauma, 15, 665-674.

SMITH, D.H., CHEN, X.H., XU, B.N., MCINTOSH, T.K. GENNARELLI, T.A., MEANEY, D.F. (1997). Characterization of Diffuse Axonal Pathology and Selective Hippocampal Damage Following Inertial Brain Trauma in the Pig. J Neuropathol Exp Neurol, 56, 822-834.

SWANSON, L.W. (1995). Mapping the Human Brain: Past, Present, and Future. TRENDS Neurosci, 18, 471-474.

UNTERHARNSCHEIDT, F.J., HIGGINS, L.S. (1969). Traumatic Lesions of Brain and Spinal Cord Due to Nondeforming Angular Acceleration of the Head. Texas Report on Biology and Medicine, 27, 127-166.

VRENKEN, H., BARKHOF, F., UITDEHAAG, B.M.J., CASTELIJNS, J.A., POLMAN, C.H., POUWELS, P.J.W. (2005). MR Spectroscopic Evidence for Glial Increases but not for Neuro-axonal Damage in MS Normal-Apprearing White Matter. Magnetic Resonance in Medicine, 53, 256-266.

XIONG, Y., MAHMOOD, A., CHOPP, M. (2013). Animal Models of Traumatic Brain Injury. Nature Reviews: Neuroscience, 14, 128-142.